

# Optimization of Abrasive Waterjet Cutting by Using the CODAS Method with Regard to Interdependent Processing Parameters

Andrzej Perec<sup>1,\*</sup> – Elżbieta Kawecka<sup>1</sup> – Aleksandra Radomska-Zalas<sup>1</sup> – Frank Pude<sup>2,3</sup>

<sup>1</sup> Jacob of Paradies University, Faculty of Technology, Poland

<sup>2</sup> Steinbeis Consulting Center High-Pressure Waterjet Technology, Germany

<sup>3</sup> Inspire AG, ETH Zurich, Switzerland

*The paper shows performance optimization effects of steel machining by abrasive water jet (AWJ). An innovative combinative distance-based assessment method (CODAS) is implemented for the optimization of cutting parameters like pump pressure, feed rate, and abrasive flow rate over cutting depth, and cut kerf surface roughness. The CODAS algorithm is among those based on measuring the distance between a scenario (in this case processing parameters in terms of performance and quality indicators) - and a certain benchmark. A benchmark is a specific hypothetical set of processing parameters devised or determined from available data. To determine the best set of process control parameters, a CODAS approach was performed with some weighting determinations. To set the initial parameters of the weights, it was proposed to calculate based on entropy weight method (EWM), that measures output value dispersion in cutting process. This technique simplifies multiple compound responses by preserving a single response.*

**Keywords:** abrasive waterjet cutting, process optimization, CODAS method, maximum cutting depth, minimum surface roughness welding, copper, metal matrix composite, boron carbide

## Highlights

- Effect of jet pressure, traverse speed, and mass flow rate of on chromium-nickel-molybdenum steel cut surface roughness was introduced.
- An optimal set of control parameters to reach the highest cutting depth and smallest surface roughness of cut kerf was determined.
- A significant abasement in the cost of the experiments by diminution the number of required tests and shortening the time to perform with high precision of results was reached.

## 0 INTRODUCTION

Optimization of control parameters is used wherever many control parameters significantly affect the result. Examples include advanced industrial processes like epoxidation [1], polymerization [2], and advanced manufacturing technologies [3] to [5].

The cutting with an abrasive waterjet (AWJ) is one of the imported methods classified as advanced manufacturing technology. It is used in many industries, including aerospace [6] and [7] automotive [8], manufacturing [9] and [10] and even in medicine [11] to [13]. However, a poorly designed process can be costly and time-consuming and optimizing it can ensure that it is as efficient, quality [14] and [15] and effective as possible.

Optimizing the control parameters of AWJ machining process is essential for achieving the desired cutting results with maximum efficiency, quality, and minimum waste. The control parameters optimization of the AWJ machining process can be achieved by using statistical methods such as design of experiments (DOE), especially Taguchi

method [16], response surface methodology (RSM) [4], artificial intelligence techniques such as neural networks and genetic algorithms, expert systems, and approximate metaheuristic methods. These methods can help identify the optimal combination of control parameters that maximize the desired cutting results, reduce waste, and improve efficiency.

There are also methods from the field of decision support or multi-criteria decision-making (MCDM) that can be successfully used to optimize the AWJ process [17] and [18].

The CODAS method is a valuable tool for solving MCDM problems. It allows to consider multiple criteria simultaneously and to balance the trade-offs between them. The method can be used in fields such as mechanical engineering, among others.

The entropy-CODAS method belongs to a multi-criteria decision-making technique used for optimization of chosen problems. It is based on the concept of entropy, which is a measure of uncertainty or disorder. The basic idea behind the method is to minimize the overall distance between the alternatives

and the ideal solution while maximizing the diversity among the alternatives.

An innovative entropy-CODAS method is implemented for the optimization of cutting depth, cut surface roughness, and angle of cut kerf was conducted.

The dimension and distribution of the used abrasive grains have a noteworthy influence on the efficiency of the cutting process by AWJ. In the cutting head takes place the intensive disintegration of abrasive materials during the creation of the abrasive jet. The disintegration of chosen abrasive materials grains was tested after forming in the cutting head [19] and [20]. Additionally, it allows to carry out recovery analysis for the recycling possibility.

Hlavacova et al. [21] introduced the study of common quality steels cut by AWJ and observed the relations concerning the mechanical characteristics of quenched steels and the chosen surface roughness parameters. The differentiation of the steel microstructure was the essential property for the cutting quality because the higher the difference in the hardness of the structural constituents in the inhomogeneous microstructure was, the higher were the surface roughness values after cutting.

Perec and Musial [22] conducted research on the use of one of the methods based on decision support, namely the VIKOR method for optimizing the parameters of wear-resistant structural steel cutting by AWJ.

However, Perec et al. [23] modeled and optimized the AWJ cutting process of tool steel based on the RSM.

Other possibility of hard material machining presented Kumari and Acherjee [24]. Authors concentrated on using criteria importance through inter-criteria correlation (CRITIC) and CODAS multicriteria decision-making methods to assess the performance of proposed approach while selecting the best advanced machining process for machining titanium from the eight most often used as AWJ machining, ultrasonic machining, chemical machining, electron beam machining, laser beam machining, electrochemical machining, electro discharge machining, and plasma arc machining. Material removal rate, shape feature, work material type, tolerance and surface finish, power requirement, and cost were the criteria used to evaluate and pick the best advanced manufacturing process.

Sivalingam et al. [25] investigated the effect of cutting process parameters on Inconel 718 alloy turning in dry and (atomized spray cutting fluid) ASCF cutting environments. The cutting parameters

were adjusted using desirability functional analysis, and two types of MCDM methods were investigated: additive ratio assessment method (ARAS) and CODAS. Both MCDM approaches yielded identical results in the form of minimal surface roughness, machining cost, power consumption and maximizing tool life, compared with dry machining.

Al-Tamimi and Sanjay [26] presented an intelligent machining model which used contemporary techniques, based on CODAS and several other as artificial neural network (ANN), adaptive neuro-fuzzy inference systems, and particle swarm optimization (ANFIS-PSO) approach for minimizing resulting force, specific cutting energy, and maximizing metal removal rate in superalloys machining.

Malaga et al. [27] presented study tended to identify the proper material for metal additive manufacturing, using MCDM approach. Information entropy method (IEM) and CODAS were taken to establish the priority order of materials. The meaningful material properties were used as the material criterium for the analysis. The decision-making techniques were deployed using real data of materials.

Sivalingam et al. [28] also presented the CODAS multi-criteria decision-making techniques and additive ratio assessment method for predicting the internal combustion engine radiator performance under 27 different operating conditions using multiwall carbon nanotubes based nanofluid. The outcomes of the regression analysis designated those substantial input factors for enhancing thermal transfer with this radiator.

Due to the difficulties in the milling of steel and the difficulty in the proper selection of cutting tools, cutting conditions and parameters of the cutting process, Abas et al. [29] performed a multi-response optimization using a CODAS method in combination with criteria importance through inter-criteria correlation (CRITIC) with satisfactory results.

The CODAS method can be also used for support of optimal selection for example supplier selection [30], wind energy plant location selection [31], dam construction material selection [32], and for sustainable material selection in construction projects with incomplete weight information [33].

Krajcarz and Spadlo [34] published experimental research of the geometric accuracy of cylindrical holes made by a high-pressure jet of water. The tests were conducted according to a three-level Box-Behnken design. Changes in the input parameters during high-pressure abrasive water jet cutting resulted in the occurrence of geometric inaccuracies. The values of

the correlation coefficient confirmed that the greatest influence of the cylindrical holes was cutting speed.

The state of art includes assorted studies on the optimization of cutting parameters, including cutting depth, cut surface roughness, and angle of cut kerf, using different methods such as entropy-CODAS, VIKOR, RSM, and multicriteria decision-making techniques like CODAS, ARAS, and desirability functional analysis. These studies focused on cutting types of materials, such as common quality steels, wear-resistant structural steel, tool steel, Inconel 718 alloy, and superalloys. Additionally, it can be observed that the CODAS method was also applied to other fields.

However, to date, the CODAS method has not been used in the optimization of AWJ machining, which defines a research gap and an area for potentially new research.

The objective of this paper is to utilize entropy-CODAS to gain an optimal combination of control parameters for maximum cutting depth and minimum surface roughness and to uncover the individual result of each control parameter on cutting depth, width of the cut kerf and its surface roughness.

## 1 MATERIALS

### 1.1 Abrasive Materials

As abrasive material the crushed rock garnet type J80A from Jinhong Mining located in Jiangsu, China was used. A sample view of grain shape and grain size distribution is presented in Fig. 1.

From the details of the mineral content shown in Table 1, more than 90 % of this type of garnet is Almandine.

Almandine belongs to the silicate mineral group as part of the larger garnet group, which includes several other types of minerals with similar crystal structures. It has the chemical formula  $\text{Fe}_3\text{Al}_2(\text{SiO}_4)_3$ , which shows it contains both iron (Fe), aluminum (Al), and silicon (Si) atoms.

Almandine is typically found in metamorphic rocks such as mica schists, gneisses, and amphibolites. It is usually red to reddish-brown in color, although it can also appear purple or black. Almandine is a hard mineral with a Mohs hardness over 7.5, making it suitable for use as an abrasive material. Other properties are shown in Table 2.

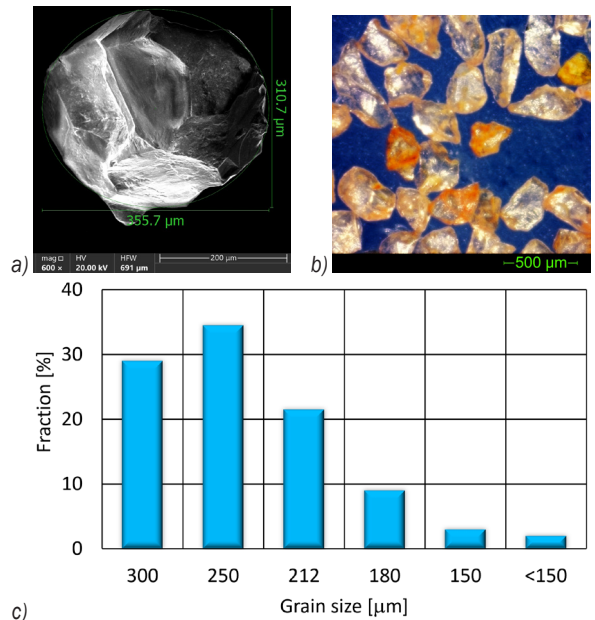


**Fig. 1.** Garnet abrasive grains: a) SEM view; b) optical microscope view; and c) grain size distribution

**Table 1.** Garnet chemical properties

Chemical composition [%]							
Fe <sub>2</sub> O <sub>3</sub>	SiO <sub>2</sub>	TiO <sub>2</sub>	Al <sub>2</sub> O <sub>3</sub>	FeO	CaO	MgO	MnO
17	39	0.05	21	8	9.5	5	0.4
Mineral content [%]							
Amandine	Ilmenite	Omphacite	Rutile	Quartz	Hornblende	Silica	
90-96	1.0	1.5	0.6	<0.1	<0.5	<0.5	

**Table 2.** Garnet physical properties

Size	Unit	Value
Density	[kg/dm <sup>3</sup> ]	3.8-4.1
Bulk gravity	[kg/dm <sup>3</sup> ]	2.3-2.4
Mohs hardness		7.5-8.0
Conductivity	[S/m]	<25
Acid solubility (HCL)	[%]	<1.0
Grain shape		Sub angular

In addition to its use as an abrasive, almandine is also used as a gemstone because of its deep red color and durability.

### 1.2 Cut Material

As target material 18CrNiMo7-6 steel for medium to high core strength engineering applications up to 62 HRC when carburized, hardened, and tempered was chosen to be cut. In this steel chromium-nickel-molybdenum were used as strengthening agents (Table 3).

**Table 3.** 18CrNiMo7-6 steel chemical composition [34]

[%]	C	Si	Mn	P	S	Cr	Ni	Mo	Cu
min	0.15	0.15	0.5	-	-	1.5	1.4	0.25	-
max	0.21	0.4	0.9	0.02	0.02	1.8	1.7	0.35	0.4

It is a high hardenability, high toughness case-hardening steel, generally supplied in the annealed condition.

It can also be used in uncarburized form as a high tensile steel, which when suitably hardened and tempered can be utilized for various applications requiring good tensile strength and toughness.

Despite difficult to cut is used extensively by all industry sectors for components and shafts requiring high surface wear resistance, high core strength and impact properties. The strength properties are presented in Table 4.

**Table 4.** 18CrNiMo7-6 steel typical mechanical properties [35] and [36]

Youngs module [GPa]	Poisson's ratio	Shear module [GPa]	Density [kg/m <sup>3</sup> ]	Tensile strength [MPa]	Yield strength [MPa]
210	0.3	80	7800	700	520

## 2 EXPERIMENTAL

### 2.1 Test Rig and Test Method

The cutting tests were carried out on the WaterJet CNC OMAX 60120 machining center (Fig. 2).

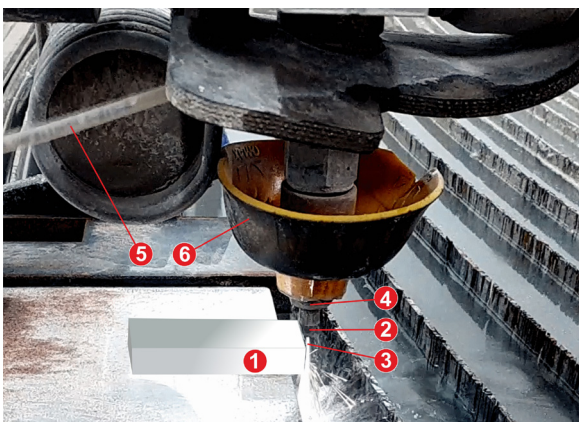


**Fig. 2.** AWJ cutting process: 1) target material, 2) focusing tube, 3) AWJ, 4) cutting head, 5) abrasive inlet, and 6) cutting head cover

The materials were cut by perpendicular to the workpiece directed AWJ, and a linear moving with a specific traverse speed. The thickness of the samples was selected to prevent complete separation of

material and an accurate determination of the cutting depth accordingly.

The process of AWJ 18CrNiMo7-6 steel cutting was conducted using the following parameters:

- pressure: 360 MPa; 380 MPa; 400 MPa,
- traverse speed: 50 mm/min; 150 mm/min and 250 mm/min,
- the abrasive flow rate: 250 g/min; 350 g/min and 450 g/min,
- abrasive material; garnet #80 (from crushed rock),
- water nozzle ID: 0.33 mm,
- focusing tube ID: 0.76 mm,
- stand-off distance: 2 mm.

#### 2.1.1 Cut Kerf Geometry

The effect of the AWJ on the material is a cut kerf. Its details are shown in Fig. 3a and the actual view in Fig. 3b. The depth of the cut groove is denoted as  $h_c$ , its width as  $W_t$ , at top and  $W_b$  at bottom, and the angle of kerf inclination as  $\delta$ .

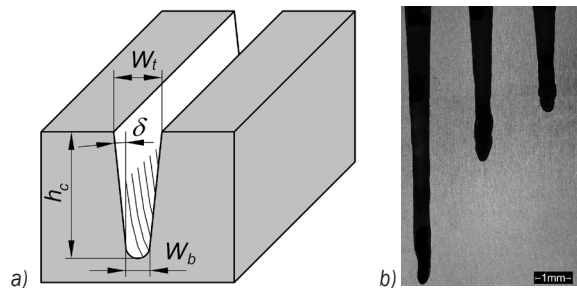


**Fig. 3.** Cut kerf dimensions: a) schematic, and b) optical microscope view

#### 2.1.2 Surface Roughness

For roughness measurement the  $Sk_u$  (kurtosis) was chosen. This parameter expands the profile (line roughness) parameter  $Rku$  three dimensionally.  $Sk_u$  is used to evaluate sharpness in the height distribution [37]. It is calculated from the following equation:

$$Sk_u = \frac{1}{Sq^4} \left( \frac{1}{A} \iint_A Z^4(x, y) dx dy \right). \quad (1)$$

This parameter concerns the height distribution and is suitable for evaluating the abrasion, when (Fig. 4):

- $Sk_u = 3$ : normal distribution,
- $Sk_u > 3$ : height distribution is sharp, and
- $Sk_u < 3$ : height distribution is even.

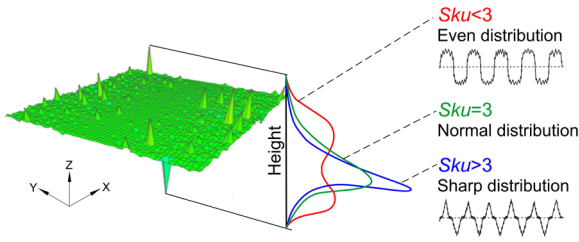


Fig. 4. *Sku roughness parameter details*

Roughness measurements were made on the high-definition Olympus DSX1000 optical microscope. The measurement area was set as  $953 \mu\text{m} \times 953 \mu\text{m}$ . Its location is shown in Fig. 4. The measurement signal was filtered with the Gaussian filter.

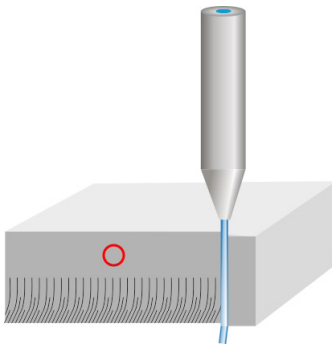


Fig. 5. *Cut kerf roughness measurement location*

## 2.2 CODAS Method

Combinative distance-based assessment (CODAS) is a multi-criteria decision-making method that was introduced in a paper by Ghorabaceet al. [38]. CODAS algorithm belongs to the class of those based on measuring the distance between a scenario (in our case, it will be the processing parameters in terms of performance and quality indicators), and a certain benchmark.

A benchmark is a certain hypothetical set of processing parameters, imagined or determined from available data. The idea behind the CODAS method is as follows: we are looking for a worst-case scenario, a negative ideal. We check how far each scenario (each set of machining parameters) is distanced from this worst-case scenario in the Euclidean sense. The farther away a set of parameters is from the counter-ideal, the better it is (and vice-versa).

In CODAS, we are interested in the negative ideal. First measure of this method is the distance of the scenario from this negative ideal is checked here, and this distance is calculated using the Euclidean metric. It is this metric that we consider the most

intuitive: the square root of the sum of the squares of the differences of the values of the corresponding coordinates.

The secondary measure is the taxicab distance which is related to the indifference space. The taxicab distance equation is grounded on the concept that the length between two points is determined by following a grid, rather than following a straight line. The equation is the sum of the absolute value of the difference of  $x$  values and the absolute value of the difference of  $y$  values.

The steps of the proposed CODAS method are presented as follows:

**Step 1.** Construct the decision-making matrix ( $\mathbf{X}$ ), shown as follows:

$$\mathbf{X} = \begin{bmatrix} x_{11} & x_{12} & \dots & x_{1m} \\ x_{21} & x_{22} & \dots & x_{2m} \\ \vdots & \vdots & \ddots & \vdots \\ x_{n1} & x_{n2} & \dots & x_{nm} \end{bmatrix}, \quad (2)$$

where  $x_{ij}$  ( $x_{ij} \geq 0$ ) denotes the performance value of  $j^{\text{th}}$  alternative on  $j^{\text{th}}$  criterion ( $i \in \{1, 2, \dots, n\}$  and  $j \in \{1, 2, \dots, m\}$ ).

**Step 2.** Calculate the normalized decision matrix. We use linear normalization of performance values as follows:

$$n_{ij} = \begin{cases} \frac{x_{ij}}{\max_i x_{ij}} & \text{if } j \in N_b \\ \frac{\min_i x_{ij}}{x_{ij}} & \text{if } j \in N_c \end{cases}, \quad (3)$$

where  $N_b$  and  $N_c$  represent the sets of benefit and cost (non-beneficial) criteria, respectively.

**Step 3.** Calculate the weighted normalized decision matrix. The weighted normalized performance values are calculated as follows:

$$r_{ij} = w_j \cdot n_{ij}, \quad (4)$$

where  $w_j$  ( $0 < w_j < 1$ ) denotes the weight of  $j^{\text{th}}$  criterion, and

$$\sum_{j=1}^m w_j = 1. \quad (5)$$

To establish the entropy factor ( $e_{i,j}$ ) exploiting the projection value of the alternative, the equation looks as follow:

$$e_{i,j} = -\frac{1}{\ln m} \sum_{i=1}^n T_{i,j} \ln T_{i,j}, \quad (6)$$

and the entropy weight of the  $j^{\text{th}}$  index is determined by equation:

$$w_i = \frac{1 - e_{i,j}}{\sum_{i=1}^n (1 - e_{i,j})} \tag{7}$$

This entropy technique was used to determine the level of individual weights. In this technique, the number of choices, and different criteria get to appraise multiple criteria optimizations on basis establishing a comparative decision matrix. If the number of choices (mass flow rate, pressure, and feed rate) getting as ‘M’, and the numbers of conditions are cutting depth surface rough-ness and angle of cut kerf get as ‘N’ then relative decision matrix having a dimension of M×N.

**Step 4.** Determine the negative-ideal solution as follows:

$$ns = [ns_j]_{1 \times m}, \tag{8}$$

$$ns_j = \min_i r_{ij}. \tag{9}$$

**Step 5.** Calculate the Euclidean and taxicab distances of alternatives from the negative-ideal solution, shown as follows:

$$E_i = \sqrt{\sum_{j=1}^m (r_{ij} - ns_j)^2}, \tag{10}$$

$$T_i = \sqrt{\sum_{j=1}^m |r_{ij} - ns_j|}. \tag{11}$$

**Step 6.** Construct the relative assessment matrix, shown as follows:

$$Ra = [h_{ik}]_{n \times m}, \tag{12}$$

$$h_{ik} = E_i - E_k + (\psi (E_i - E_k) \times (T_i - T_k)), \tag{13}$$

where  $k \in \{1, 2, \dots, n\}$  and  $\psi$  denotes a threshold function to recognize the equality of the Euclidean distances of two alternatives, and is defined as follows:

$$\psi(x) = \begin{cases} 1 & \text{if } |x| \geq \tau \\ 0 & \text{if } |x| < \tau \end{cases} \tag{14}$$

where  $\tau$  is the threshold parameter that can be set by decisionmaker. It is suggested to set this parameter at a value between 0.01 and 0.05. If the difference between Euclidean distances of two alternatives is less than  $\tau$ , these two alternatives are also compared by the taxicab distance. In this study for the calculations was used  $\tau=0.02$ .

**Step 7.** Calculate and rank the alternatives according to the decreasing values of assessment score ( $H_i$ ):

$$H_i = \sum_{k=1}^n h_{ik}. \tag{15}$$

The alternative with the highest  $H_i$  factor is the best choice among the alternatives.

### 3 RESULTS AND DISCUSSION

The results shown in Table 5, while Table 6 displays the calculation effects of the normalizing, weighted normalized performance values, Euclidean and taxicab distances of alternatives, assessment score factor and their ranks.

**Table 5.** Cutting process tests results

No	AFR	p	Vp	hc	Sku
1	250	360	50	7.48	2.57
2	250	380	150	5.09	3.01
3	250	400	250	2.93	2.63
4	350	360	150	4.99	3.72
5	350	380	250	3.06	2.65
6	350	400	50	8.70	2.46
7	450	360	250	3.31	2.66
8	450	380	50	7.59	3.83
9	450	400	150	4.89	2.65

**Table 6.** CODAS coefficients and rank

No	Ri(b)	Ri(nb)	Ei	Ti	H	Rank
1	0.55	0.35	0.35	0.36	1.23	2
2	0.37	0.29	0.17	0.31	-0.42	5
3	0.22	0.34	0.11	0.35	-1.20	9
4	0.37	0.24	0.15	0.25	-0.58	6
5	0.23	0.33	0.10	0.35	-1.02	8
6	0.64	0.36	0.44	0.38	2.03	1
7	0.24	0.33	0.11	0.35	-1.00	7
8	0.56	0.23	0.34	0.25	1.14	3
9	0.36	0.33	0.18	0.35	-0.36	4

The calculated  $H_i$  represents the better the status, the higher values it takes. Out of all  $H_i$  value in the frame of the reference sequence is the best combination of parameters and is thereby recommended.

For these tests, the recommended values for control parameters (highlighted row in Table 6) are as follows:

- abrasive feed rate: 350 g/min,
- pressure: 400 MPa,
- traverse speed: 50 mm/min.

Examples of the effects of machining with the control parameters optimally determined by this method are shown in Fig. 5. Numerous traces of erosion of the material by abrasive grains were observed here. They become visible in the form of parallel machining footprints. They are visible especially in Fig. 6a in the form of parallel lines located on macrograins, at an acute angle. There is no chaotic arrangement of traces on adjacent grains, which indicates good cutting conditions.

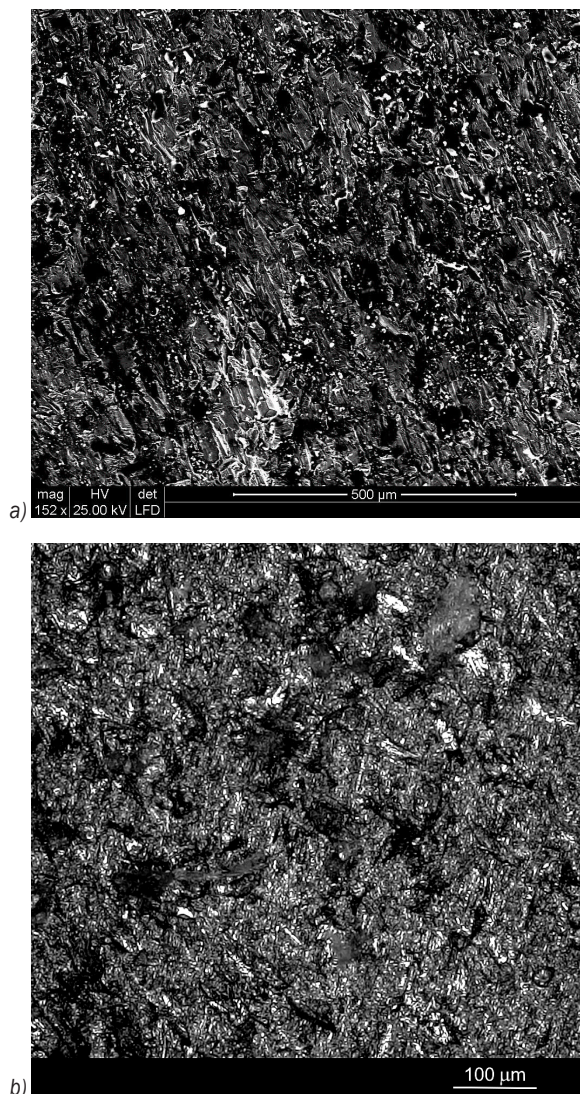


**Fig. 6.** Cut kerf surface at optimal conditions: a) SEM view, and b) optical microscope view

#### 4 CONCLUSIONS

The conducted research confirmed the equity of applying the method in multi-criteria optimization

of the 18CrNiMo7-6 steel cutting process by AWJ. The CODAS method transforms the multiple characteristics of cutting process into the individual  $H_i$  coefficient, which significantly simplifies the computation. The CODAS method determines the ranks of evident from computational results by optimal machining variable combination.

Optimal condition from cutting depth and roughness surface was achieved at following control parameters:

- abrasive feed rate: 350 g/min,
- pressure: 400 MPa,
- traverse speed: 50 mm/min.

Future studies will be conducted on the impact of other control parameters.

#### 5 NOMENCLATURES

$X$	decision-making matrix,
$AFR$	abrasive flow rate, [g/min]
$p$	pressure, [MPa]
$Vp$	traverse speed, [mm/min]
$hc$	depth of cut, [mm]
$N_b$	set of benefit criteria,
$N_c$	set of cost (non-beneficial) criteria,
$n_{ij}$	normalized decision matrix,
$ns$	negative solution,
$Sku$	surface roughness factor (curtosis), [ $\mu\text{m}$ ]
$R_a$	relative assessment matrix value,
$r_{ij}$	weighted normalized performance value,
$Ei$	Euclidean distances of alternatives,
$Ti$	taxicab distances of alternatives,
$H_i$	assessment score factor,
$\psi$	threshold function.

#### 6 REFERENCES

- [1] Radomska-Zalas, A. (2022). The AHP method in the optimization of the epoxidation of allylic alcohols. *Procedia Computer Science*, vol. 207, p. 456-464, DOI:10.1016/j.procs.2022.09.100.
- [2] Radomska-Zalas, A., Fajdek-Bieda, A. (2021). IT support for the optimization of the epoxidation of unsaturated compounds on the example of the TOPSIS method. I. Czarnowski; R. J. Howlett; L. C. Jain (Eds.). *Intelligent Decision Technologies* (vol. 238), Springer Singapore, p. 297-307, DOI:10.1007/978-981-16-2765-1\_25.
- [3] Sabotin, I., Tristo, G., Valentinčič, J. (2020). Technical model of micro electrical discharge machining (EDM) milling suitable for bottom grooved micromixer design optimization. *Micromachines*, vol. 11, no. 6, art. ID 594, DOI:10.3390/mi11060594.
- [4] Perec, A., Radomska-Zalas, A., Fajdek-Bieda, A., Pude, F. (2022). Process optimization by applying the response

- surface methodology (RSM) to the abrasive suspension water jet cutting of phenolic composites. *Facta Universitatis, Series: Mechanical Engineering*, Online first: <http://casopisi.junis.ni.ac.rs/index.php/FUMechEng/article/view/10193>, DOI:10.22190/FUME211123010P.
- [5] Pellegrini, G., Ravasio, C. (2020). A sustainability index for the micro-EDM drilling process. *Journal of Cleaner Production*, vol. 247, art. ID 119136, DOI:10.1016/j.jclepro.2019.119136.
- [6] Pahuja, R., Ramulu, M. (2019). Abrasive water jet machining of Titanium (Ti6Al4V)-CFRP stacks - A semi-analytical modeling approach in the prediction of kerf geometry. *Journal of Manufacturing Processes*, vol. 39, p. 327-337, DOI:10.1016/j.jmapro.2019.01.041.
- [7] Lehocká, D., Klichová, D., Foldyna, J., Hloch, S., Hvizdoš, P., Fides, M., Botko, F. (2017). Comparison of the influence of acoustically enhanced pulsating water jet on selected surface integrity characteristics of CW004A copper and CW614N brass. *Measurement*, vol. 110, p. 230-238, DOI:10.1016/j.measurement.2017.07.005.
- [8] Hlavacek, P., Zlamal, T., Sitek, L. (2018). Abrasive water jet drilling of cooling holes in aeroengines: preliminary experimental study. *MM Science Journal*, vol. 2018, no. 01, p. 2218-2222, DOI:10.17973/MMSJ.2018\_03\_201771.
- [9] Hloch, S., Souček, K., Svobodová, J., Hromasová, M., Müller, M. (2022). Subsurface microtunneling in ductile material caused by multiple droplet impingement at subsonic speeds. *Wear*, vol. 490-491, art. ID 204176, DOI:10.1016/j.wear.2021.204176.
- [10] Valíček, J., Drzik, M., Hloch, S., Ohlidal, M., Miloslav, L., Gombar, M., Radvanska, A., Hlavacek, P., Palenikova, K. (2007). Experimental analysis of irregularities of metallic surfaces generated by abrasive waterjet. *International Journal of Machine Tools & Manufacture*, vol. 47, no. 11, p. 1786-1790, DOI:10.1016/j.ijmactools.2007.01.004.
- [11] Nag, A., Hloch, S., Dixit, A.R.; Pude, F. (2020). Utilization of ultrasonically forced pulsating water jet decaying for bone cement removal. *The International Journal of Advanced Manufacturing Technology*, vol. 110, no. 3-4, p. 829-840, DOI:10.1007/s00170-020-05892-9.
- [12] Hreha, P., Hloch, S., Magurova, D., Valicek, J., Kozak, D., Harnicarova, M., Rakin, M. (2010). Water jet technology used in medicine. *Tehnicki Vjesnik*, vol. 17, no. 2, p. 237-240.
- [13] Hloch, S., Foldyna, J., Sitek, L., Zeleňák, M., Hlaváček, P., Hvizdos, P., Kl'oc, J., Monka, P., Monkova, K., Kozak, D., Magurová, D. (2013). Disintegration of bone cement by continuous and pulsating water jet. *Tehnicki Vjesnik*, vol. 20, p. 593-598.
- [14] Stolárik, G., Nag, A., Petrů, J., Svobodová, J., Hloch, S. (2021). Ultrasonic pulsating water jet peening: Influence of pressure and pattern strategy. *Materials*, vol. 14, no. 20, art. ID 6019, DOI:10.3390/ma14206019.
- [15] Hloch, S., Srivastava, M., Nag, A., Müller, M., Hromasová, M., Svobodová, J., Kruml, T., Chlupová, A. (2020). Effect of pressure of pulsating water jet moving along stair trajectory on erosion depth, surface morphology and microhardness. *Wear*, vol. 452-453, art. ID 203278, DOI:10.1016/j.wear.2020.203278.
- [16] Perec, A. (2016). Abrasive suspension water jet cutting optimization using orthogonal array design. *Procedia Engineering*, vol. 149, p. 366-373, DOI:10.1016/j.proeng.2016.06.680.
- [17] Perec, A., Radomska-Zalas, A. (2022). WASPAS optimization in advanced manufacturing. *Procedia Computer Science*, vol. 207, p. 1193-1200, DOI:10.1016/j.procs.2022.09.175.
- [18] Radomska-Zalas, A., Perec, A., Fajdek-Bieda, A. (2019). IT support for optimisation of abrasive water cutting process using the TOPSIS method. *IOP Conference Series: Materials Science and Engineering*, vol. 710, art. ID 012008, DOI:10.1088/1757-899X/710/1/012008.
- [19] Perec, A. (2021). Research into the disintegration of abrasive materials in the abrasive water jet machining process. *Materials*, vol. 14, no. 14, art. ID 3940, DOI:10.3390/ma14143940.
- [20] Perec, A. (2017). Disintegration and recycling possibility of selected abrasives for water jet cutting. *DYNA*, vol. 84, no. 203, p. 249-256, DOI:10.15446/dyna.v84n203.62592.
- [21] Hlavacova, I., Sadilek, M., Vanova, P., Szumilo, S., Tyc, M. (2020). Influence of steel structure on machinability by abrasive water jet. *Materials*, vol. 13, no. 19, art. ID 4424, DOI:10.3390/ma13194424.
- [22] Perec, A., Musial, W. (2021). Multiple criteria optimization of abrasive water jet cutting using entropy-VIKOR approach. S. Hloch, D. Klichová, F. Pude, G. M. Krolczyk, S. Chattopadhyaya (Eds.). *Advances in Manufacturing Engineering and Materials II*, Springer International Publishing, Cham, p. 50-62, DOI:10.1007/978-3-030-71956-2\_5.
- [23] Perec, A., Radomska-Zalas, A., Fajdek-Bieda, A., Kawecka, E. (2022). Efficiency of tool steel cutting by water jet with recycled abrasive materials. *Materials*, vol. 15, no. 11, art. ID 3978, DOI:10.3390/ma15113978.
- [24] Kumari, A., Acherjee, B. (2022). Selection of non-conventional machining process using CRITIC-CODAS method. *Materials Today: Proceedings*, vol. 56, p. 66-71, DOI:10.1016/j.matpr.2021.12.152.
- [25] Sivalingam, V., Poogavanam, G., Natarajan, Y., Sun, J. (2022). Optimization of atomized spray cutting fluid eco-friendly turning of Inconel 718 alloy using ARAS and CODAS methods. *The International Journal of Advanced Manufacturing Technology*, vol. 120, no. 7-8, p. 4551-4564, DOI:10.1007/s00170-022-09047-w.
- [26] Al-Tamimi, A.A., Sanjay, C. (2023). Intelligent systems to optimize and predict machining performance of Inconel 825 alloy. *Metals*, vol. 13, no. 2, art. ID 375, DOI:10.3390/met13020375.
- [27] Malaga, A.K., Agrawal, R., Wankhede, V.A. (2022). Material selection for metal additive manufacturing process. *Materials Today: Proceedings*, vol. 66, p. 1744-1749, DOI:10.1016/j.matpr.2022.05.272.
- [28] Sivalingam, V., Ganesh Kumar, P., Prabakaran, R., Sun, J., Velraj, R., Kim, S.C. (2022). An automotive radiator with multi-walled carbon-based nanofluids: A study on heat transfer optimization using MCDM techniques. *Case Studies in Thermal Engineering*, vol. 29, art. ID 101724, DOI:10.1016/j.csite.2021.101724.

- [29] Abas, M., Alkahtani, M., Khalid, Q. S., Hussain, G., Abidi, M. H., Buhl, J. (2022). Parametric study and optimization of end-milling operation of AISI 1522H steel using definitive screening design and multi-criteria decision-making approach. *Materials*, vol. 15, no. 12, art. ID 4086, DOI:10.3390/ma15124086.
- [30] Badi, I., Shetwan, A.G., Abdulshahed, A.M. (2017). Supplier selection using combinative distance-based assessment (CODAS) method for multi-criteria decision-making. *SSRN Electronic Journal*, p. 397-407, DOI:10.2139/ssrn.3177276.
- [31] Karaşan, A., Boltürk, E., Kahraman, C. (2019). A novel neutrosophic CODAS method: Selection among wind energy plant locations. *Journal of Intelligent & Fuzzy Systems*, vol. 36, no. 2, p. 1491-1504, DOI:10.3233/JIFS-181255.
- [32] Ijadi Maghsoodi, A., Ijadi Maghsoodi, A., Poursoltan, P., Antucheviciene, J., Turskis, Z. (2019). Dam construction material selection by implementing the integrated SWARA-CODAS approach with target-based attributes. *Archives of Civil and Mechanical Engineering*, vol. 19, no. 4, p. 1194-1210, DOI:10.1016/j.acme.2019.06.010.
- [33] Roy, J., Das, S., Kar, S., Pamučar, D. (2019). An extension of the CODAS approach using interval-valued intuitionistic fuzzy set for sustainable material selection in construction projects with incomplete weight information. *Symmetry*, vol. 11, no. 3, art. ID 393, DOI:10.3390/sym11030393.
- [34] Krajcarz, D., Spadlo, S. (2016). Influence of the process conditions on the diameter of cylindrical holes produced by abrasive water jet cutting. *METAL 2016: 25<sup>th</sup> Anniversary International Conference on Metallurgy and Materials*, p. 1462-1467.
- [35] Ovako Steel Navigator (2023). 18CrNiMo7-6, from <https://steelnavigator.ovako.com/steel-grades/18crnimo7-6/>, accessed 2023-03-08.
- [36] Interlloy (2023). 4317 Case Hardening Steel | Interlloy | Engineering Steels + Alloys, Interlloy Engineering Steels and Alloys, from <http://www.interlloy.com.au/our-products/case-hardening-steels/x4317-case-hardening-steel/>, accessed 2023-03-08.
- [37] Surface Roughness Measurement-Parameters | Olympus. (2023), from <https://www.olympus-ims.com/en/metrology/surface-roughness-measurement-portal/parameters/#:~:focus=areal-method>, accessed 2023-07-19.
- [38] Ghorabae, M.K., Zavadskas, E.K., Turskis, Z., Antucheviciene, J. (2016). A new combinative distance-based assessment (CODAS) method for multi-criteria decision-making. *Economic Computation and Economic Cybernetics Studies and Research*, vol. 50, no. 3, p. 25-44.